An Investigation of Process Parameters Effects on Void Formation in Fluxless Solder Paste for Power Module Packaging Applications via Formic Acid Vacuum Reflow Technology

Ji, Liangzheng; Guo, Wenwu; Zhang, Guoqi; Zhang, Jing; Liu, Pan

DOI
10.1109/ICEPT63120.2024.10668644

Publication date
2024

Document Version
Final published version

Published in
2024 25th International Conference on Electronic Packaging Technology, ICEPT 2024

An Investigation of Process Parameters Effects on Void Formation in Fluxless Solder Paste for Power Module Packaging Applications via Formic Acid Vacuum Reflow Technology

Liangzheng Ji
Academy for Engineering and Technology
Fudan University
Shanghai, China
21110860032@m.fudan.edu.cn

Wenwu Guo
Heraeus Materials Technology Shanghai Ltd.
Shanghai, China
wenwu.guo@heraeus.com

Guoqi Zhang
Electronic components, Technology, and Materials
Delft University of Technology
Delft, Netherlands
g.q.zhang@tudelft.nl

Jing Zhang*
Heraeus Materials Technology Shanghai Ltd.
Shanghai, China
j.zhang@heraeus.com

Pan Liu*
Academy for Engineering and Technology
Fudan University
Shanghai, China
panliu@fudan.edu.cn

2024 25th International Conference on Electronic Packaging Technology (ICEPT) | 979-8-3503-5380-8/24/$31.00 ©2024 IEEE | DOI: 10.1109/ICEPT63120.2024.10668644

***Abstract*—The soldering process, essential for electrical and mechanical connections in the microelectronics industry, is crucial for IGBT die attachment as well. This paper investigates the impact of the vacuum reflow process on IGBT assembly using fluxless solder paste activated by formic acid. The paste demonstrates excellent print quality, formability, and consistent solder joint formation. Achieving satisfactory wetting, it compares favorably to traditional solder materials. Key optimized parameters include reflow temperature profiles, activation, and vacuum conditions, such as preheat time, time above liquid (TAL), peak temperature, formic acid concentration, and vacuum ratio. Crucially, formic acid's concentration and activation duration play significant roles in reducing void percentages, effectively decreasing voids from 7.5% to as low as 1%. Vacuum pressure also critically influences void behavior, with reductions in pressure resulting in increased void percentages from 1% to a high of 30%. This study underscores the potential of fluxless solder methodology as a sustainable and economic advancement in the power electronics industry.**

***Keywords*—IGBT chip assembly, Fluxless solder paste, Formic acid vacuum reflow, Void ratio**

I. INTRODUCTION

The Insulated Gate Bipolar Transistor (IGBT) module, essential for power electronics, boasts significant advantages such as high efficiency and low power loss, which have facilitated its widespread adoption in sectors including electric vehicles and wind power [1-2]. Crucial to the IGBT's reliable performance is the solder layer, a vital interface that ensures electrical continuity and aids thermal dissipation. Traditional soldering methods, utilizing flux-enhanced solder pastes for oxide removal and surface cleaning [3], necessitate subsequent cleaning steps to prevent flux-induced corrosion and prepare for further assembly stages like wire bonding. However, these additional steps can reduce manufacturing efficiency and increase both complexity and costs. In response to these challenges, industry practices have shifted towards formic acid vacuum reflow technology combined with solder preforms to mitigate void formation and enhance the solder layer's integrity [4]. Although these methods decrease the presence of voids, they also introduce operational complexities that may affect production throughput.

Recent innovations have ushered in the era of fluxless solder pastes, now gaining traction in academia and industry. Utilized in a reducing environment of hydrogen or formic acid, these pastes significantly improve the solder's wettability on substrates by reducing metal oxides without traditional flux [5-8]. Formic acid-enriched nitrogen, preferred for its effective oxide reduction at lower temperatures than hydrogen, has become a favored activator in fluxless soldering, compatible with existing reflow soldering processes and manageable in terms of health risks [9-11].

Furthermore, research by Du and colleagues into void formation provides critical insights, although detailed studies on void dynamics in fluxless soldering are lacking. This paper aims to bridge this gap by analyzing the impact of vacuum reflow processing parameters on fluxless solder paste for IGBT module assembly. This comprehensive investigation modifies reflow temperature profiles and vacuum conditions to minimize solder voids, thereby enhancing the reliability of IGBT modules.

Firstly, the printability and wettability of fluxless solder paste were explored, providing a consistent basis for the subsequent study of voids. The void performance across various profiles of fluxless solder paste focused on refining several key parameters. These parameters include reflow temperature profiles, activation settings, and specific vacuum conditions such as preheat time, time above liquid (TAL), peak temperature, formic acid concentration, and vacuum ratio. Notably, the concentration and activation duration of formic acid are identified as pivotal factors in reducing void percentages, successfully minimizing void occurrence from 7.5% down to as low as 1%. Additionally, vacuum pressure has a critical impact on void behavior, with reductions in pressure correlating with increases in void percentages, ranging from 1% up to a peak of 30%. This research highlights the potential of fluxless solder methodology as a sustainable and economically viable advancement in the power electronics sector, suggesting a significant paradigm shift towards enhanced productivity and reliability in manufacturing.

II. Experimental Methodology

A. Preparation of Soldered Samples

In this study, a formic acid-assisted vacuum reflow process was utilized to prepare the soldered samples for voiding behavior study. The preparation process involved stencil printing to deposit fluxless solder paste (from Heraeus Group) onto the Direct Bond Copper (DBC) substrate and placing dummy dies over the deposited paste with dimensions of 5 mm x 5 mm x 0.2 mm and 10 mm x 10 mm x 0.2 mm, respectively, to simulate the actual IGBT chips. The backside of the chips had an Ag/Ni coating with a thickness of over 1 µm. The resulting sandwich structure was subjected to the reflow process. The specific reflow parameters required are discussed in the Results and Discussion section. A Pink Vadu 2000 oven was utilized for the process. Fig. 1 depicts the schematic of the fluxless solder process, which consists of five phases. In the first phase, vacuum-inert gas purging was conducted to eliminate oxygen from the oven. Nitrogen gas was introduced into the chamber to create a protective atmosphere and reduce residual oxide content. During this phase, the oven was heated. The second phase involved a temperature ramp-up until reaching the soaking temperature. The third phase, known as the soak phase or activation phase, introduced formic acid-enriched nitrogen as the gaseous activator into the chamber. Formic acid was dispensed from a glass container by bubbling nitrogen onto its surface, enabling the release of formic acid into the reflow chamber. The formic acid reacted with the solder spheres, forming metal formate that facilitated the removal of oxide layers and promoted welding in the subsequent stage. This transformation of Sn oxide to Sn formate occurred between 150 °C and 190 °C. The soak time for fluxless soldering in this study ranged from a few seconds to several seconds. Next, the sandwich structure was heated to the melting temperature, surpassing the liquidus temperature of the solder alloy. Once the peak temperature was reached, the cooling phase commenced, allowing the solder joint to solidify.

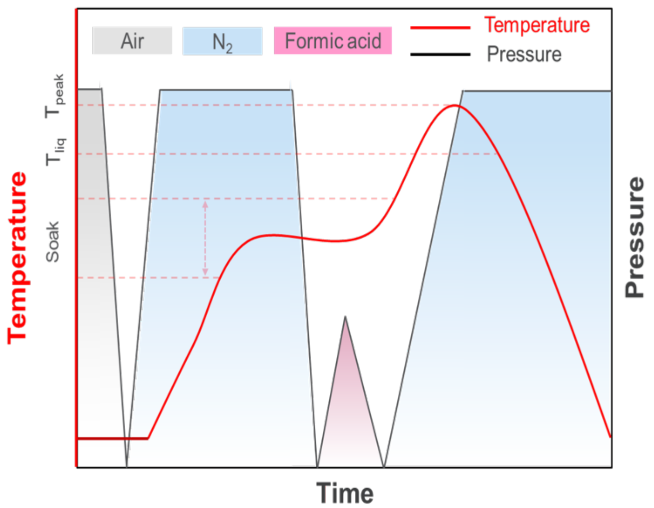

Fig. 1. Schematic diagram of the fluxless solder paste reflow profile.

B. Inspection and performance analysis

After printing and soldering the solder pads were inspected by a solder paste inspection (SPI, Parmi) to check the printability of the paste onto the solder pads, and optical microscope (Keithley VHX-900F) to record the paste printing performance. The solder joint inspection after soldering can be done using both non-destructive and destructive analysis. The non-destructive analysis involves X-ray analysis, where X-ray images of solder joints are taken to analyze the voiding. The voids impact IGBT chip thermal dissipation, a crucial factor for power modules. To assess the wettability of fluxless solder paste in comparison to conventional solder paste and solder preform, a destructive test was performed as follows: Each type of solder paste was printed onto Direct Bond Copper (DBC) substrates in a predefined pattern and subjected to a reflow process. After reflow, cross-sectional samples were prepared for detailed analysis. Optical photographs of these samples were captured to measure the wetting angles of the solder joints, providing comparative insights into their wetting behaviors.

III. Results and Discussion

A. Printability of solder paste

Proper solder paste deposition enables the formation of robust solder joints, ensuring excellent electrical conductivity and mechanical strength. Moreover, uniform solder paste application minimizes the occurrence of voids, which can create thermal hotspots, compromise electrical performance, and lower the overall reliability of the assembly. In this study, the printing behavior of fluxless solder paste was studied first. The experiments conducted in this study involved the printing of fluxless solder paste on substrates using stencil printing. Two different stencil opening dimensions were utilized: 5 mm x 5 mm and 10 mm x 10 mm. As Fig. 2 (a) shows, the print performance of the solder paste using both stencil opening sizes was excellent. The solder paste exhibited good formability and did not show any instances of missing or misaligned solder paste, ensuring consistent and reliable solder joint formation. Furtherly, As shown in Fig. 2 (b), the results of the SPI inspection revealed that the coverage area of the solder paste was 100%, indicating that the solder paste was applied uniformly across the intended areas. This suggests that the printing process achieved complete coverage of the desired regions on the substrate. The high-quality printing of fluxless solder paste provided a solid foundation for subsequent optimization studies, specifically targeting the reduction of voids and improving overall solder joint performance. The absence of apparent defects or irregularities in the printed solder paste further validated the efficacy and potential viability of fluxless solder paste as an alternative soldering solution.

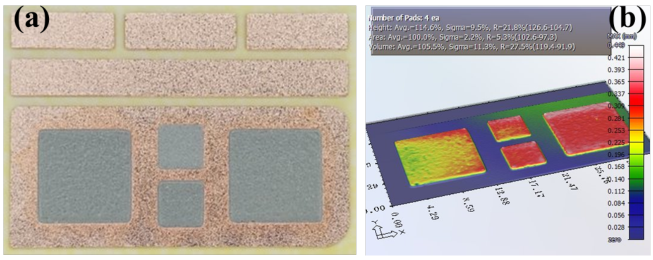

Fig. 2. (a) optical image of fluxless solder paste after printing, (b) Solder paste distribution map detected by SPI.

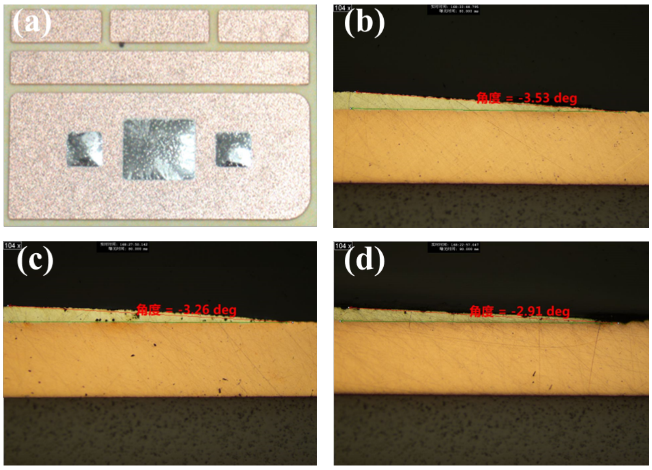

Fig. 3. (a) optical image of fluxless solder paste after soldering, contact angle formed between solder joint and DBC substrate of (b) fluxless solder paste, (c) solder preform, (d) traditional flux-based solder paste.

B. Wettability of solder materials

In our study, we conducted a comparison of the contact angles between traditional solder paste, solder preforms, and fluxless solder paste. Fig. 3 (a) depicts a photograph of fluxless solder paste after reflowing on a DBC substrate. The contact angle measurement was performed to evaluate the wetting behavior of the solder on the substrate surface. After a cross-section analysis, using an optical microscope, the contact angle (θ) was measured for both the fluxless solder paste and the reference solder paste. Fig. 3 (b) shows the contact angle of the fluxless solder paste, which measured 3.53 degrees. In comparison, Fig. 3 (c) displays the contact angle of the solder preform, which measured 3.26 degrees, while Fig. 3 (d) shows the contact angle of the traditional solder paste, which measured 2.91 degrees. Based on these results, it can be concluded that the fluxless solder paste exhibits a similar wetting behavior compared to commercial flux-based solder pastes. The contact angle measurements indicate that the fluxless solder paste demonstrates good surface wetting characteristics, identical to the traditional solder paste and solder preforms. These findings suggest that the fluxless solder paste shows promising wetting properties, thus being a suitable alternative for reliable soldering applications. Overall, the comparison of contact angles highlights the effectiveness of the fluxless solder paste in achieving satisfactory wetting and bonding between the solder and the substrate, corroborating its potential as a viable alternative to traditional soldering materials.

C. The void performance across various profiles

Voids play a vital role in the packaging of Insulated Gate Bipolar Transistors (IGBTs). These empty spaces or cavities that are formed within the solder joints during the soldering process have significant implications for the reliability and performance of the IGBT module. Understanding the mechanisms behind the void formation and the subsequent behavior of these voids during the soldering process is essential for optimizing manufacturing processes and ensuring the long-term functionality of IGBTs. During the soldering process, voids can arise due to various factors, such as trapped gases, inconsistencies in solder paste deposition, and the release of volatiles from the solder material. The formation and behavior of voids are influenced by several factors, including surface tension, and wetting characteristics

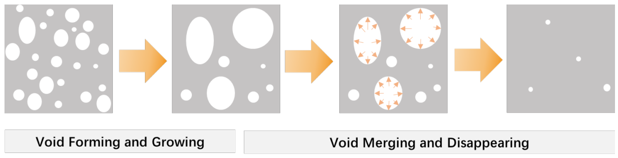

Fig. 4. Schematic diagram of void formation and disappearance process.

As depicted in Fig. 4, the solder voids formation involves the following steps. Initially, small voids may form due to the release of gases from the solder paste, as well as the evaporation of binders and solvents. These initial voids tend to grow as the heating continues, facilitated by the reduction of surface tension. This growth is supported by two main mechanisms: buoyancy-driven growth, which occurs due to the upward movement of gas within the molten solder, and diffusion-driven growth, driven by the diffusion of gas molecules through the molten solder.

The application process of fluxless solder paste necessitates the use of formic acid-assisted vacuum reflow, which involves three primary factors that directly influence the formation and behavior of voids: temperature, reactivity (derived from formic acid), and vacuum pressure. These factors directly impact the formation and behavior of voids. Higher temperatures facilitate the release of trapped gases, reducing void formation. The reactivity of formic acid, an activator in the paste, helps remove oxide layers, enhancing wetting and reducing voids. Vacuum pressure removes gases, minimizing void formation and improving solder joint reliability. Optimization of these factors ensures reliable and robust joints in electronic components.

In this study, we comprehensively investigated the effects of various process parameters on void formation in solder joints. Profile A acts as the base profile, all the parameters were optimized based on that. These parameters included variations in reflow peak temperature, time above liquidus (TAL) duration, soak time, formic acid concentration, activation time, and vacuum ratio. The soldering process was applied to dummy chips measuring 5mm x 5mm and 10mm x 10mm on DBC substrates.

TABLE I. VARIOUS REFLOW PROFILES

Profile	**A**	**B**	**C**	**D**	**E**	**F**
Soaking time (sec)	210	208	210	214	211	243
Peak temperature (°C)	239	249	230	236	237	236
Time Above Liquid (sec)	105	113	104	119	93	105
FA pressure (kPa)	50	50	50	50	50	50
FA duration (sec)	67	67	67	67	67	67
Vacuum ratio (kPa * sec)	0.2* 30	0.2* 30	0.2* 30	0.2* 30	0.2* 30	0.2* 30
Profile	**G**	**H**	**I**	**J**	**K**	**L**
Soaking time (sec)	183	211	215	210	218	211
Peak temperature (°C)	240	238	239	240	241	242
Time Above Liquid (sec)	108	101	105	107	101	104
FA pressure (kPa)	50	70	30	50	50	50
FA duration (sec)	67	98	39	82	60	60
Vacuum ratio (kPa * sec)	0.2* 30	0.2* 30	0.2* 30	0.2* 30	10* 30	20* 30

The relationship between temperature and void ratio

As depicted in Fig. 5, post-reflow images of profiles A-G are presented. The corresponding numerical values are shown in Fig. 6. Fig. 5 (b) shows that as the peak temperature increases to 249°C, there is a slight increase in voids on the 10 mm x 10 mm chip, while no significant change is observed on the 5mm x 5mm chip compared to Fig. 5 (a) and Fig. 5 (c). However, when the temperature is lowered to 230°C, irregular voids appear on one of the 10mm x 10mm chips, and there is a noticeable increase in void size on the 5 mm x 5 mm chip, reaching 6.2%. This could be attributed to the lower temperature, where the vaporization force of the bubbles is reduced, leading to a hindered release of trapped gases. Additionally, Fig. 5 (d) and Fig. 5 (e) demonstrate that variations in the TAL duration do not significantly affect the void size. Although slight changes are observed, it suggests that there is minimal correlation between TAL and void formation. Further investigation into the effect of soak time reveals that prolonged or shortened soaking times result in a notable increase in void size (as shown in Figs. 6 (f) and (g)). This could be attributed to the inhibition of solvent and binder evaporation in the fluxless system. When the soaking time is extensive, excessive evaporation of solvents and binders can prevent the effective activation of formic acid due to the absence of the necessary carrier environment, leading to inadequate wetting and void formation. The results indicate that temperature and soak time have some impact on void formation, though not substantial, while Time Above Liquid (TAL) shows minimal correlation with void size.

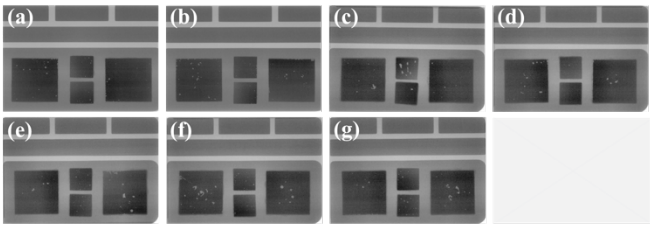

Fig. 5. The X-ray picture after reflowing through (a) profile A, (b) profile B, (c) profile C, (d) profile D, (e) profile E, (f) profile F, (g) profile G.

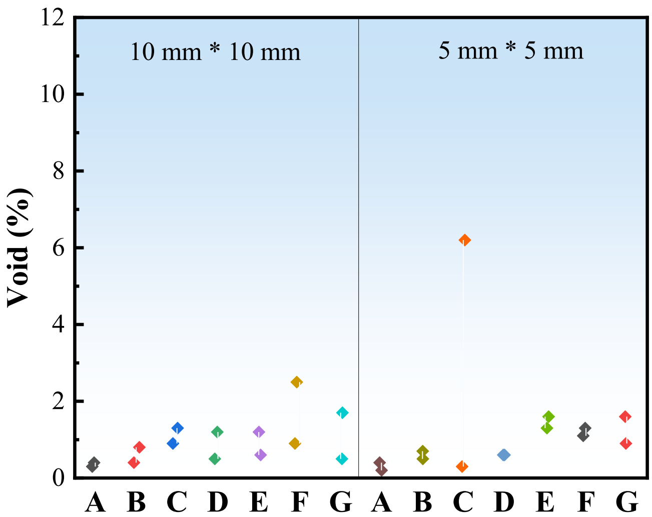

Fig. 6. Voiding distribution on 5 mm * 5 mm and 10 mm * 10 mm dies through profiles A-G.

The relationship between activation and void ratio

As shown in Fig. 7, post-reflow images of profiles A, H, I, and J are presented. The corresponding numerical values are shown in Fig. 8. In the experimental setup, variations in formic acid pressure result in variations in time. By directly comparing the formic acid pressure and duration, Fig. 7 (h) demonstrates that when the formic acid concentration changes from 50 kPa with a duration of 67 s to 70 kPa with a duration of 98 s, the void values remain around 1%, regardless of whether it is a 5mm x 5mm or 10mm x 10mm chip. Conversely, when the formic acid concentration changes to 30 kPa with a duration of 39s, significant changes in void formation occur. As shown in Fig. 7 (i), on the 5mm x 5mm chip, the void percentage increases to between 2.9% and 7%, while on the 10mm x 10mm chip, it rises to between 3.8% and 7.5%. From another perspective, without changing the formic acid pressure, extending the duration of formic acid treatment (Fig. 7 (j)) yields similar results to increasing the formic acid pressure, with void percentages remaining around 1%. Formic acid plays a crucial role as an activator in the fluxless soldering process. Regardless of whether the concentration increases, or the duration extends, both result in an increase in the amount of formic acid within the system, providing more reactivity. This suggests that in the fluxless soldering process, the reactivity of formic acid is critical for void formation. Increasing either the formic acid concentration or the treatment duration enhances the effectiveness of the activator, leading to consistent void percentages around 1%. These findings highlight that formic acid concentration and duration play significant roles in void formation during the fluxless soldering process. The concentration and reactivity of formic acid are crucial factors that contribute to the successful reduction of voids.

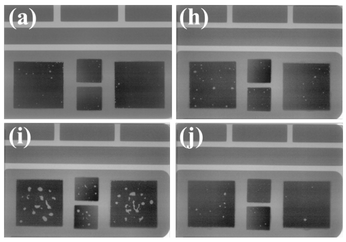

Fig. 7. The X-ray picture after reflowing through (a) profile A, (h) profile H, (i) profile I, (j) profile J.

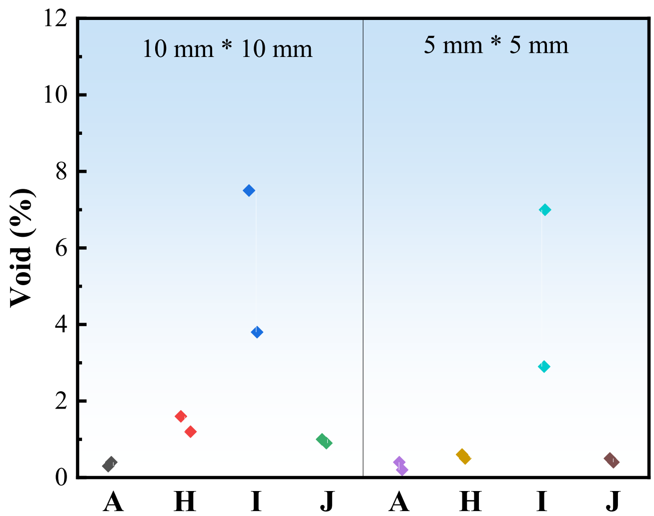

Fig. 8. Voiding distribution on 5 mm * 5 mm and 10 mm * 10 mm dies through profiles A, H, I, and J.

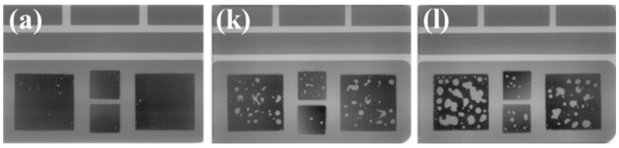

Fig. 9. The X-ray picture after reflowing through (a) profile A, (k) profile K, (l) profile L.

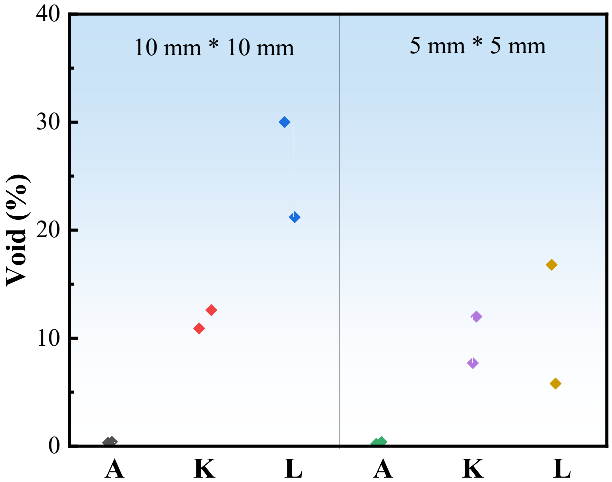

Fig. 10. Voiding distribution on 5 mm * 5 mm and 10 mm * 10 mm dies through profiles A, K, and L.

The relationship between vacuum ratio and void ratio

Voids can exhibit accelerated expulsion when subjected to sufficient external forces. In this study, vacuum technology was applied to facilitate void expulsion. As a reference group, a vacuum pressure of 0.2 kPa with a duration of 30 s demonstrated excellent void performance, with void percentages maintained at around 1% for both chip sizes. To further investigate the impact of vacuum pressure, two additional Design of Experiments (DOEs) were designed: one with a vacuum pressure of 10 kPa and a duration of 30 s (Fig. 9 (k)), and another with a vacuum pressure of 20 kPa and a duration of 30 s (Fig. 9 (l)), as detailed in Fig. 10. It can be observed that, for both the 5mm x 5mm and 10mm x 10mm chips, as the vacuum pressure decreases, there is a noticeable increase in void percentage. In Fig. 9 (k), with a vacuum pressure of 10 kPa and a duration of 30 s, the void percentage on the 5 mm x 5 mm chip increases to between 7.7% and 12%, while on the 10mm x 10mm chip, it rises to between 12.6% and 10.9%. In Fig. 9 (l), with a vacuum pressure of 20 kPa and a duration of 30 s, the void percentage on the 5 mm x 5 mm chip increases to between 5.8% and 16.8%, and on the 10 mm x 10 mm chip, it rises to between 21.2% and 30%, representing a significant deterioration. These findings demonstrate the significant influence of vacuum pressure on void behavior. As the vacuum pressure weakens, there is a notable increase in void percentage, indicating the importance of vacuum pressure in facilitating void expulsion during the fluxless soldering process.

IV. Conclusion

In conclusion, this study systematically investigated the printability and wettability of fluxless solder paste, laying a solid foundation for an in-depth analysis of void dynamics within IGBT module assembly. The investigation into the void performance of fluxless solder paste emphasized the critical refinement of several parameters including reflow temperature profiles, activation settings, and specific vacuum conditions such as preheat time, time above liquid (TAL), peak temperature, formic acid concentration, and vacuum ratio.

The findings demonstrate that while temperature and soak time modestly influence void formation, these factors are not the primary determinants of void size. In contrast, the concentration and activation duration of formic acid is shown to significantly facilitate void reduction, effectively decreasing the void occurrence from 7.5% to as low as 1%. Additionally, the study underscores a critical relationship between vacuum pressure and void behavior, revealing that reductions in vacuum pressure directly lead to increases in void percentages, with observed ranges spanning from 1% to as high as 30%.

This research advocates for optimally adjusting soldering parameters using fluxless solder methodology to potentially revolutionize IGBT module production, making it more sustainable, economically viable, and efficient in the power electronics industry.

Acknowledgment

The authors thank the Fudan University and Heraeus cooperation project in this work.

References

[1] A. Abuelnaga, M. Narimani, A.S. Bahman, A Review on IGBT Module Failure modes and Lifetime Testing, IEEE Access, vol. 9, pp. 9643-9663, 2021.

[2] T. Chen, J. Zhang, J.M. Fei, B.B. Zhang, N.N. Rong, Research on Vacuum Soldering Technology of Military IGBT Module, 2019 20th International Conference on Electronic Packaging Technology (ICEPT), 2019.

[3] N. Mohan, S. Langer, G. Elger, Fluxfree solder paste and process for standard SMD components, 2022 IEEE 9th Electronics System-Integration Technology Conference (ESTC), pp. 163-168, 2022.

[4] M. Du, Q. Guo, H. Wang, Z. Ouyang, K. Wei, An Improved Cauer Model of IGBT Module: Inclusive Void Fraction in Solder Layer, IEEE Transactions on Components, Packaging, and Manufacturing Technology, vol.10, no. 8, pp. 1401-1410, 2020.

[5] S. He, Y. Bi, Y.-A. Shen, Z. Chen, G. Yue, C. Hu, H. Nishikawa, Contact angle analysis and intermetallic compounds formation between solders and substrates under formic acid atmosphere, Journal of Advanced Joining Processes, vol. 6, pp. 100118, 2022.

[6] S. He, R. Gao, J. Li, Y.A. Shen, H. Nishikawa, In-situ observation of fluxless soldering of Sn-3.0Ag-0.5Cu/Cu under a formic acid atmosphere, Materials Chemistry and Physics, vol. 239, pp. 122309, 2020.

[7] S. He, R. Gao, Y.A. Shen, J. Li, H. Nishikawa, Wettability, interfacial reactions, and impact strength of Sn–3.0Ag–0.5Cu solder/ENIG substrate used for fluxless soldering under formic acid atmosphere, Journal of Materials Science, vol. 55, no. 7, pp. 3107-3117, 2020.

[8] S. He, Y.-A. Shen, B. Xiong, F. Huo, J. Li, J. Ge, Z. Pan, W. Li, C. Hu, H. Nishikawa, Behavior of Sn-3.0Ag-0.5Cu solder/Cu fluxless soldering via Sn steaming under formic acid atmosphere, Journal of Materials Research and Technology vol. 21, pp. 2352-2361, 2022.

[9] M. Samson, V. Oberson, I. Paquin, C. Fortin, D. Wright, Fluxless Chip Join Process Using Formic Acid Atmosphere in a Continuous Mass Reflow Furnace, 2016 IEEE 66th Electronic Components and Technology Conference (ECTC), pp. 574-579, 2016.

[10] A. Hanss, G. Elger, Residual free solder process for fluxless solder pastes, Soldering & Surface Mount Technology vol. 2, pp. 3, 2018.

[11] F. Conti, A. Hanss, O. Mokhtari, S.K. Bhogaraju, G. Elger, Formation of tin-based crystals from a SnAgCu alloy under formic acid vapor, New Journal of Chemistry, vol. 42, no. 23, pp. 19232-19236, 2018.